JCTC Journal of Chemical Theory and Computation

The Exchange-Energy Density Functional Based on the Modified Becke-Roussel Model

Hideaki Takahashi,* Ryohei Kishi, and Masayoshi Nakano

Division of Chemical Engineering, Department of Materials Engineering Science, Graduate School of Engineering Science, Osaka University, Toyonaka Osaka 560-8531, Japan

Received August 10, 2009

Abstract: In this paper, we present a simple numerical approach to implement the modified Becke−Roussel (mBR) model for the purpose of developing an exchange density functional suitable for applications to atoms or molecules. Three steps constitute our approach. The first step is to model the exchange hole with the mBR distribution with the form of $\rho_{X\sigma}^{mBR} = (\alpha/\pi)^{3/2} \exp(-\alpha r^2)$ at each reference point, where α and r represent, respectively, the diffuseness and the distance of the model exchange hole from the reference point. We propose an iterative procedure to determine the values (α, r) during the Kohn−Sham DFT calculation. Second, we make a GGA correction to the functional obtained in the first step by adopting the conventional GGA formula to the gradients of the spin density as well as the mBR exchange hole (mBR-GGA). In the third step, mBR-GGA is combined with Dirac's exchange functional to restore the exchange energy at the homogeneous electron gas limit (mBR-hyb). We demonstrate that the exchange energy densities of the mBR-based methods obey the $-1/r$ asymptotic behaviors by virtue of the fact that the electron density in a hydrogenic atom is used as a prototypical exchange hole. Furthermore, we perform several test calculations for the properties of small molecules. For atomization energies for 35 molecules in the G2 set, the mean absolute deviation (MAD) with respect to the experiment is estimated to be 4.9 kcal/mol by the mBR-hyb functional, which is much smaller than the value of PBE functional (7.7 kcal/mol). The MAD for the enthalpies of formation of 68 molecules in the G3 set is evaluated as 9.4 kcal/mol by the present method, while that is given as 18.7 kcal/mol by the PBE functional. These results suggest the possibility of the present functional based on the mBR model for the applications to atoms or molecules.

1. Introduction

The density functional for the exact exchange energy of homogeneous electron gas was first formulated by Dirac in an attempt to establish a purely density-functional approximation for the electronic energy of a system.[1] The exchange functional was then introduced into the effective Hamiltonian in place of the exact exchange potential by Slater for the purpose of simplifying the Hartree−Fock method.[2] Later, this approach was reinterpreted within the rigorous framework of the Kohn−Sham density functional theory (KS-DFT)[3] and was validated as the local density approximation (LDA). The possibility of gradient corrections to the inhomogeneous electron density in a real system was first suggested by Hohenberg and Kohn[4] and afterward successfully taken into account by the method termed generalized gradient approximations (GGA).[5,6] The simplest form of the gradient correction is based on the lowest order gradient expansion,[7] which is, however, divergent in the limit of low electron density. In 1988, Becke proposed a nondivergent form of the functional satisfying correct asymptotic behavior of the exchange energy density (B88),[8] where one adjustable parameter was introduced in the correction term. Later in 1996, Perdew, Burke, and Ernzerhof developed an empirical-parameter-free exchange functional by imposing

* To whom correspondence should be addressed. E-mail: takahasi@cheng.es.osaka-u.ac.jp.

10.1021/ct900416x
Published on Web 02/01/2010

some physical constraints (PBE).[9] These exchange formulas in combination with correlation functionals achieved almost comparable accuracies to some molecular orbital theories considering the electron correlations. The success of the GGA correction encouraged subsequent improvements of the functional. In 1993, Becke proposed to mix the exact exchange potential to incorporate the kinetic correlation energy[10] in the functional through the adiabatic connection method. Perdew et al. made remarkable improvements in the computation of the molecular atomization energies by the method termed meta-GGA that includes the kinetic energy density and/or the Laplacian of the electron density in the functional.[11] A number of functionals are also being developed to compensate for other deficiencies inherent in the LDA-based KS-DFT such as the self-interaction error (SIE)[5,6,12,13] or the lack of long-range behavior of the exchange potential.[6,14,15] As shown in the Figure 1 in ref 16, each step in the development is often compared to various rungs of "Jacob's ladder" that may lead to the heaven of chemical accuracy.

Here, we pose a question whether the ladder in which LDA is regarded as the first rung is the only way to improve the exchange-correlation functionals. The exchange hole distribution in the homogeneous electron gas is spherically symmetric around the reference electron as a matter of course. In a bulk system, such hole behavior simulated by LDA gives a reasonable description for the real exchange hole. The bulk system has no boundary of the electron cloud, and hence, the exchange hole is always localized to some extent in the vicinity of the reference electron. On the contrary, in a finite molecular system, the exchange hole resides at the molecule even when the reference electron is placed far apart from the molecule. This is the origin of the fact that the exact exchange energy density as well as the exchange potential obeys $-1/r$ asymptotic behavior given that r is the distance between the reference electron and the molecule. Nevertheless, the hole depth within the LDA description decreases exponentially as r increases because of the exponential decay of the electron density. This results in a well-known unsatisfactory short-range behavior of the exchange energy density.[8] Thus, there is still room to consider another candidate for the exchange functional for the applications to atoms and molecules instead of the conventional route that begins with the homogeneous electron gas.

In this respect, Becke and Roussel (BR) proposed a unique exchange hole model for *inhomogeneous* systems.[17,18] They introduced the density of a 1s electronic wave function in a hydrogenic atom as a model of the exchange hole in molecular systems. The nuclear charge of the atom (which determines the diffuseness of the hole) and the distance of the hole from the reference electron are determined by imposing a condition that the model hole realizes the behavior of the spherically averaged exchange hole of the real system near the reference point. The exchange energy density is, then, computed as the Coulomb interaction between the reference electron and the exchange hole. The BR approach seems to be a natural choice for the exchange-hole model for the systems suffering serious inhomogeneity, such as atoms or molecules. It is worth noting that the long-range nature of the exchange energy density is fully restored in the BR model since it takes the hydrogenic atom as a prototypical system. In the subsequent developments by Becke et al., the BR model was utilized in the functional as a device to simulate the static correlations[19] or to generate the dispersion interactions.[20] The drawback of the BR approach is that the functional derivative with respect to the electron density cannot be evaluated explicitly, and hence, the variational potential appearing in the KS equation cannot be obtained as suggested in ref 18. In the writing of this paper, we noticed that Neumann et al. provided an efficient numerical technique to implement the BR functional into the self-consistent calculations in the KS-DFT with LCAO (linear combination of atomic orbitals) basis sets.[21,22] However, its realization in the computation with the real-space grids method[23] as well as the plane wave basis would still remain to be difficult. Although the BR model has many encouraging properties, so far there have been only a small number of numerical examples to the best of our knowledge.[18,22,24] In addition, in most cases in these studies, the one-electron wave functions were given at the outset, and the BR model was only used to evaluate the exchange energies for the given electron densities. In the present work, to quest for a new route to the exchange functional for practical applications, we propose a simple numerical approach efficient for any choice of the basis set within the framework of the BR model. Our strategy to implement the BR approach is to express the nuclear charge of the hydrogenic atom (or equivalently the exponent of the hole) as a functional of the electron density at the reference point. Then, the distance between the reference point and the hole is determined by ensuring that the hole density coincides with the electron density at the reference point. Second, the gradient correction to this scheme is also taken into consideration by utilizing the conventional GGA formula.

The organization of this paper is as follows. Section 2 is devoted to describing the details of the methodology. We first present a concise review for the original BR approach. Then, our approach is presented for the numerical implementation of the modified BR model in KS-DFT. The computational details for the test calculations utilizing the real-space grids approach are presented in section 3. We examine in section 4 the behaviors of the exchange energy density as well as the exchange potential with respect to the variation of the distance between the reference point and a molecule of interest. We also study the efficiency of the method by computing several properties of the small molecules such as atomization energy, ionization potentials, etc. In section 5, we provide a summary and conclusions to discuss the possibilities of the BR-model-based exchange functional.

2. Methodology

2.1. Exchange Hole Based on the Becke−Roussel Model. In the Becke−Roussel (BR) approach,[18] the exchange hole distribution $\rho_{X\sigma}(R)$ for spin σ in a molecule is

represented by a Slater function, which is a normalized 1s orbital density of a hydrogenic atom:

$$\rho_{X\sigma}^{BR}(R) = \frac{\alpha^3}{8\pi}\exp(-\alpha R) \quad (1)$$

In eq 1, R is the distance of the center of the hole from the reference electron. α specifies the diffuseness of the hole and is related to the nuclear charge of the hydrogenic atom. Provided that α and R are known for any given reference point $\mathbf{r}$, the exchange energy density $U_{X\sigma}^{BR}(\mathbf{r})$ based on the BR approach is expressed by the Coulomb interaction between the reference electron and the exchange hole distribution; thus,

$$U_{X\sigma}^{BR}(\mathbf{r}) = -\int_0^\infty ds \frac{1}{s}\int_{\Omega_s} \rho_{X\sigma}^{BR}(\mathbf{r}+\mathbf{s})\, d\mathbf{s} \quad (2)$$

In eq 2, Ω_s denotes the integration over a sphere of radius s centered at the reference point $\mathbf{r}$. The energy of eq 2 represents the exchange energy per electron in the BR model at the point $\mathbf{r}$ and is often referred to as exchange energy density. Note that $U_{X\sigma}^{BR}(\mathbf{r})$ is only dependent on the values (α, R). The exchange energy for spin σ is, then, given by using $U_{X\sigma}^{BR}(\mathbf{r})$; thus,

$$E_{X\sigma}^{BR} = \frac{1}{2}\int d\mathbf{r}\, \rho_{X\sigma}(\mathbf{r})\, U_{X\sigma}^{BR}(\mathbf{r}) \quad (3)$$

For the evaluation of the exchange energy, it is required to obtain the values (α, R) in eq 1 at every reference point. Becke and Roussel proposed to use these values as parameters to mimic the realistic exchange hole by a proper fitting at each reference point. Explicitly, the values (α, R) are determined by imposing the condition that the spherical average of the Taylor expansion of the model exchange hole around the reference point reproduces that of the real system up to the second order term of the expansion. In the following, we briefly review the procedure to determine (α, R). The exact spherically averaged exchange hole near the reference point $\mathbf{r}$ is expressed by

$$\rho_{SA-X\sigma}(\mathbf{r}, s) = \rho_\sigma(\mathbf{r}) + \frac{1}{6}(\nabla^2\rho_\sigma - 2\gamma D_\sigma)s^2 + \cdots \quad (4)$$

where s is the radius of the sphere centered at $\mathbf{r}$. $\rho_\sigma(\mathbf{r})$ in eq 4 is the electron density with σ spin, and D_σ is given by

$$D_\sigma = \tau_\sigma - \frac{1}{4}\frac{(\nabla\rho_\sigma)^2}{\rho_\sigma} \quad (5)$$

where τ_σ is the kinetic energy density and is defined as

$$\tau_\sigma = \sum_i |\nabla\phi_{\sigma i}|^2 \quad (6)$$

γ in eq 4 is the parameter to be used in later reference, and the equality $\gamma = 1$ holds in the exact expression.

For the exchange hole model defined by eq 1, the spherically averaged exchange hole is analytically expressed by a function of the variables (α, R) as

$$\rho_{SA-X\sigma}^{BR}(\alpha, R; s) = \frac{\alpha}{16\pi Rs}[(\alpha|R-s|+1)\exp(-\alpha|R-s|) - (\alpha|R+s|+1)\exp(-\alpha|R+s|)] \quad (7)$$

By equating the first two coefficients of the Taylor expansion of eq 7 to those of the real system given by eq 4, we obtain two equations:

$$\alpha^3\exp(-\alpha R) = 8\pi\rho_\sigma \quad (8)$$

and

$$\alpha^2 R - 2\alpha = 6RQ_\sigma/\rho_\sigma, Q_\sigma = \frac{1}{6}(\nabla^2\rho_\sigma - 2\gamma D_\sigma) \quad (9)$$

Then, they lead to the following equation with the definition of $x = \alpha R$,

$$\frac{x\exp(-2x/3)}{x-2} = \frac{2}{3}\pi^{2/3}\frac{\rho_\sigma^{5/3}}{Q_\sigma} \quad (10)$$

The variable x in eq 10 is obtained by using the Newton−Raphson scheme, from which the parameters (α, R) are determined. Importantly, eq 10 assures the existence of a unique and positive root x for all conditions. The exchange energy density at reference point $\mathbf{r}$ is, then, given by

$$\begin{aligned} U_{X\sigma}^{BR}(\mathbf{r}) &= -4\pi\int_0^\infty ds\, \rho_{SA-X\sigma}^{BR}(\alpha, R; s)s \\ &= -\left(1 - \exp(-R) - \frac{1}{2}R\exp(-R)\right)/R \end{aligned} \quad (11)$$

It is readily verified that $U_{X\sigma}^{BR}(\mathbf{r})$ behaves as $-1/r$ when $\mathbf{r}$ is placed far apart from the molecular system. It is worth noting that one of the important features to be fulfilled by the approximate exchange functional is, thus, naturally incorporated in the BR functional from the outset by virtue of the fact that the atomic electron density is chosen as a prototypical system.

2.2. Modified Becke-Roussel Model and Its Implementation. Here, we introduce a modified Becke−Roussel (mBR) model where the exchange hole is modeled by a Gaussian function instead of the Slater type one as given by eq 1. Recently, such a modification was also suggested by Bahmann and Ernzerhof,[25] who mixed the mBR model with LDA by a switching factor, where the missing cusp of the hole distribution is traded for the simplified integrals. In the present work, we introduce the mBR model for the purpose of suiting the BR model to the Kohn−Sham equation that utilizes pseudopotentials. The exact exchange hole at a given reference point is described in terms of the one-electron wave functions, and hence, the exchange-hole distribution reflects the behavior of the one-electron wave functions to some extent. Since the point of the BR approach is to express the spherical average of the hole distribution by that of the atomic orbital density, a Gaussian function will be well suited to mimic the behavior of the pseudo-wave functions of which variation near the nuclei are forced to be sufficiently smooth. On the contrary, the Slater function of eq 1 is appropriate for modeling the exchange hole in all-electron calculations where the wave functions have cusps

near the nuclei. In the present work, we propose a numerical approach for implementing both the mBR and the original BR methods. Within the mBR model, the exchange hole is represented by a normalized Gaussian function:

$$\rho_{X\sigma}^{mBR}(R) = \left(\frac{\alpha}{\pi}\right)^{3/2}\exp(-\alpha R^2) \tag{12}$$

The notations in eq 12 are synonymous with those in eq 1. As discussed for the original BR model in section 2, the determination of the parameters (α, R) is also crucial in the mBR approach. We propose here a simpler numerical approach to obtain these values than those proposed in refs 18 and 21. At first, we consider two limiting situations for a reference electron. In case 1, the reference electron is assumed to be placed at the position where the electron density of the system has its maximum value ρ_σ^{max} ($\rho(\mathbf{r}) = \rho_\sigma^{max}$). And in case 2, it is assumed that the reference point is placed far apart from the molecular system ($\rho(\mathbf{r}) \cong 0$). The concept of the Fermi orbital suggests that the behavior of the exchange hole is dominated by the orbital that gives a major contribution to the total density at the reference point. Hence, it is reasonable to consider that the exchange-hole distributions for the reference electrons in cases 1 and 2 are characterized by the core orbital and the HOMO of the system, respectively. Then, for these two limiting situations, it is possible to estimate approximately the parameters (α, R) in eq 12. For case 1, the center of the exchange hole may coincide well with the position of the reference electron, which implies that the variable R in eq 12 can be taken as zero. Further, we impose a physical constraint that the exchange-hole density at the reference point is exactly the same with the electron density

$$\rho_{X\sigma}^{mBR}(R)|_{R=0} = \rho_\sigma^{max} \tag{13}$$

This condition can be easily verified by taking $s = 0$ in the expansion of eq 4. Then, we have

$$\alpha_1 = \pi\rho_\sigma^{max\ 2/3} \tag{14}$$

where α_1 denotes specifically the value of α for case 1. As for the reference electron in the opposite situation (case 2), the exchange hole obeys the asymptotic form as derived in refs 26 and 27; thus,

$$\lim_{R\to\infty} \rho_{X\sigma} = \exp(-\alpha'_0 R) \tag{15}$$

Equation 15 is consistent with the fact that the wave function decays exponentially in the asymptotic region. More importantly, the exponent α_0' in eq 15 can be approximately related to the ionization potential I as follows:

$$\frac{1}{2}\alpha'^2_0 = I \tag{16}$$

According to the proof given in ref 28, the eigenvalue ϵ_{HOMO} of the exact Kohn−Sham equation is identical to $-I$. Hence, α_0' in eq 16 can be approximated as

$$\alpha'_0 = (-2\varepsilon_{HOMO})^{1/2} \tag{17}$$

To employ the mBR model for describing the asymptotic hole distribution, the Slater function with exponent α_0' given by eq 17 has to be fitted by a Gaussian function. As shown in ref 29, the value α_0, defined as the exponent for case 2, can be derived from α_0' by least-squares fitting and the scaling relation; thus,

$$\alpha_0 = \alpha_0^{1.0} \times \alpha'^2_0 \tag{18}$$

where $\alpha_0^{1.0}$ is the exponent of the Gaussian function fitted to the Slater one with the exponent $\alpha_0' = 1.0$. Thus, we can deduce approximately the exponents α_1 and α_0 with $R = 0$ and $R \to \infty$ corresponding to the opposite situations $\rho(\mathbf{r}) = \rho_\sigma^{max}$ and $\rho(\mathbf{r}) = 0$, respectively. Here, we should note that the use of ϵ_{HOMO} leads to an undesirable consequence that the size consistency cannot be fulfilled. To show this, we consider a complex of two monomers with different HOMO energies at a large separation. Then, the HOMO energy of the complex will be the same as the constituent molecule with the larger eigenvalue. Hence, the complex does not have the same energy as the separated fragments. Thus, our present approach violates the size consistency. This limitation should be kept in mind in simulating the dissociation processes.

For the determination of the exponent α in eq 12 for the intermediate reference point $\mathbf{r}$, which satisfies $0 < \rho_\sigma(\mathbf{r}) < \rho_\sigma^{max}$, we introduce the interpolation

$$\frac{\alpha - \alpha_0}{\alpha_1 - \alpha_0} = \left(\frac{\rho_\sigma(\mathbf{r})}{\rho_\sigma^{max}}\right)^p \tag{19}$$

where p is the scaling parameter. Once the exponent α is, thus, obtained, the distance R between the reference point and the exchange hole can be simply derived from the relation $\rho_\sigma(\mathbf{r}) = \rho_{X\sigma}^{mBR}(R)$ as

$$R = \left(-\frac{1}{\alpha}\log\left(\left(\frac{\pi}{\alpha}\right)^{3/2}\rho_\sigma(\mathbf{r})\right)\right)^{1/2} \tag{20}$$

Since the exchange energy density $U_{X\sigma}^{mBR}$ is the Coulomb interaction between the reference electron and the exchange hole, $U_{X\sigma}^{mBR}$ is simply given by

$$U_{X\sigma}^{mBR}(\mathbf{r}) = -\frac{1}{R}\mathrm{Erf}(-\alpha^{1/2}R) \tag{21}$$

with the definitions of eqs 19 and 20. Then, the exchange energy $E_{X\sigma}^{mBR}$ of the system based on the mBR model is given by

$$E_{X\sigma}^{mBR} = \frac{1}{2}\int d\mathbf{r}\ \rho_\sigma(\mathbf{r})\ U_{X\sigma}^{mBR}(\mathbf{r}) \tag{22}$$

It should be noted that the functional of eq 22 fulfills the important property that the exchange hole contains just one electron. Furthermore, it is ensured by the construction that the exchange-hole density at the reference point is exactly equal to the electron density (i.e., the first term of the expansion of eq 4 is ensured). Here, we also note that it can be readily proved there exists no real value of R for $p > 2/3$ in eq 19. In other words, we can choose p as a scaling parameter to control the diffuseness of the exchange hole with respect to the magnitude of the spin density. At first,

we check the performance of the functional with the critical value of $p = 2/3$ to assess the efficiency of the present approach based on the BR model and then optimize the parameter to refine the functional (see details in section 2.4).

For the implementation of the mBR approach in the Kohn−Sham equation, it is necessary that the exchange potential $v_{X\sigma}^{mBR}(\mathbf{r})$ is obtained by the derivative of $E_{X\sigma}^{mBR}$ with respect to the density $\rho_\sigma(\mathbf{r})$,

$$v_{X\sigma}^{mBR}(\mathbf{r}) \equiv \frac{\delta E_{X\sigma}^{mBR}(\mathbf{r})}{\delta \rho_\sigma} = \frac{1}{2}\left(U_{X\sigma}^{mBR}(\mathbf{r}) + \rho_\sigma(\mathbf{r}) \frac{\partial U_{X\sigma}^{mBR}(\mathbf{r})}{\partial \rho_\sigma} \right) \tag{23}$$

As described in the previous paragraph, the exchange functional $E_{X\sigma}^{mBR}$ defined by eqs 19−22 contains the parameters α_1 and α_0. We note that these parameters are also dependent on the electron density; however, the derivatives of the exponents α_1 and α_0 with respect to $\rho_\sigma(\mathbf{r})$ are unavailable. Here, we adopt the following numerical approach to determine these parameters iteratively. Analytical expression $\tilde{v}_{X\sigma}^{mBR}(\mathbf{r})$ for the derivative $\delta U_{X\sigma}^{mBR}(\mathbf{r})/\delta\rho_\sigma$ can be readily obtained by supposing that the values α_1 and α_0 are fixed. Then, we consider solving the following Kohn−Sham equation with the exchange potential $v_{X\sigma}^{mBR\prime}$,

$$\left[-\frac{1}{2}\nabla^2 + V_{H-ps}(\mathbf{r}) + \tilde{v}_{X\sigma}^{mBR}(\mathbf{r}) + v_{c\sigma}(\mathbf{r}) \right] \varphi_{i\sigma}(\mathbf{r}) = \varepsilon_i \varphi_{i\sigma}(\mathbf{r}) \tag{24}$$

where V_{H-ps} is the sum of the Hartree and pseudopotentials, and $v_{c\sigma}$ denotes the correlation potential. The solution of eq 24 leads to the electron density $\rho_\sigma(\mathbf{r})$ and ϵ_{HOMO}, from which we derive new values of α_1 and α_0 by eqs 14, 17, and 18. Using the renewed α_1 and α_0, we reconstruct the potential $\tilde{v}_{X\sigma}^{mBR}(\mathbf{r})$ and solve eq 24. This procedure is continued until the parameters α_1 and α_0 converge. We confirm in practice that the renewal of these values at every SCF step is sufficient for the convergence. This iterative approach will give rise to an instability in the SCF procedure to some extent; however, our test calculation shows a satisfying convergence rate as demonstrated in section 4.1. Thus, we obtain a simplified procedure based on the BR model for describing the exchange energy. In closing this paragraph, it should be noted that we are not guaranteed to have the proper exchange potential even at the convergence since it is not possible to obtain the correct Kohn−Sham eigenvalues.

So far, we have discussed the practical implementation of the mBR approach that is efficient for the calculations with the plane-wave basis and real-space grid methods utilizing pseudopotentials. Here, we also illustrate a method along this line for the original BR model with the form of eq 1. As for the exponent α_1' of the Slater-type exchange hole for the situation of case 1, we have

$$\alpha'_1 = 2(\pi\rho_\sigma^{max})^{1/3} \tag{14'}$$

as the counterpart of eq 14 for the Gaussian function. The exponent α_0' for case 2 is directly determined by eq 17 when we employ the Slater function. Then, the exponent α' for the intermediate reference point can be determined as

$$\frac{\alpha' - \alpha'_0}{\alpha'_1 - \alpha'_0} = \left(\frac{\rho(\mathbf{r})}{\rho_{max}} \right)^{p'} \tag{19'}$$

We note that the scaling parameter p' in eq 19′ can also be considered as an adjustable parameter which should satisfy $0 \le p' \le 1/3$. In accord with the choice of $p = 2/3$ in eq 19 for the case of the Gaussian-type exchange hole, p' is taken as 1/3 for eq 19′. Then, the distance r' between the reference point and the center of the Slater-type hole is expressed as

$$R' = -\frac{1}{\alpha'} \log\left(\frac{8\pi}{\alpha'^3} \rho_\sigma(\mathbf{r}) \right) \tag{20'}$$

The exchange energy density $U_{X\sigma}^{BR}$ is exactly expressed in the form given by eq 11. The subsequent procedure for the SCF calculation for the solution of the Kohn−Sham equation is essentially parallel to that for the mBR model.

2.3. Gradient Correction to Modified Becke−Roussel Model. The exchange functional introduced in the previous section is originated from the BR model and has an important property that the exchange energy density obeys $-1/r$ asymptotic behavior for the reference electron placed far apart from the molecule. It is obvious that this advantage is attributed to the nature of the atomic electron density chosen as a model exchange hole. However, our simplified approach does not involve the information of the gradient of the electron density in its functional. And, hence, it gives exactly the same value of the exchange energy density at two different points as far as they have the same electron density. Here, we propose a method to incorporate the gradient correction into the mBR approach (mBR-GGA) by utilizing the conventional GGA formalism. In the following, we present the formulation for the mBR-GGA approach. At first, we consider the expansion of the spherically averaged exchange hole for the mBR model that is completely parallel to eq 4; thus,

$$\rho_{SA-X\sigma}^{mBR}(\mathbf{r}, s) = \rho_{X\sigma}^{mBR}(\mathbf{r}) + \frac{1}{6}(\nabla^2 \rho_{X\sigma}^{mBR} - 2\gamma D_\sigma^{mBR}) s^2 + \cdots \tag{25}$$

The notational conventions in eq 25 are, of course, common with those in eq 4, except that the superscripts mBR are attached to each function. The exact spherically averaged exchange hole $\rho_{SA-X\sigma}(\mathbf{r},s)$ can be formally written as

$$\rho_{SA-X\sigma}(\mathbf{r}, s) = \rho_{SA-X\sigma}^{mBR}(\mathbf{r}, s) + (\rho_{SA-X\sigma}(\mathbf{r}, s) - \rho_{SA-X\sigma}^{mBR}(\mathbf{r}, s)) \tag{26}$$

By substituting the expansions given by eqs 4 and 25 into eq 26, we obtain an exact expression for $\rho_{SA-X\sigma}(\mathbf{r},s)$ as

$$\rho_{SA-X\sigma}(\mathbf{r}, s) = \rho_{SA-X\sigma}^{mBR}(\mathbf{r}, s) + \left(\left(\frac{1}{6}(\nabla^2 \rho_\sigma - 2\gamma D_\sigma) s^2 + \ldots \right) - \left(\frac{1}{6}(\nabla^2 \rho_{X\sigma}^{mBR} - 2\gamma D_\sigma^{mBR}) s^2 + \ldots \right) \right) \tag{27}$$

The relation of $\rho_{X\sigma}^{mBR}(\mathbf{r}) = \rho_\sigma(\mathbf{r})$ is used in taking the subtraction in the parentheses of eq 26. The exchange energy contribution due to the term $\rho_{SA-X\sigma}^{mBR}(\mathbf{r},s)$ in the right-hand side of eq 27 is what we discussed in section 2.2 and explicitly given by eq 22. The s^2 terms in the parentheses of eq 27 are the leading terms of the gradient corrections for

the electron density of the real system and the exchange hole distribution of the mBR model. Here, it should be reminded that the GGA approach is constructed to evaluate approximately the contribution due to the s^2 term in the gradient expansion. Our method to evaluate eq 27 is to compute gradient corrections in the parentheses by employing the available GGA exchange functionals $E_{X\sigma}^{GGA}$ such as B88 and PBE; thus,

$$E_{X\sigma}^{mBR\text{-}GGA} = E_{X\sigma}^{mBR} + (E_{X\sigma}^{GGA}[\rho_\sigma, \nabla\rho_\sigma] - E_{X\sigma}^{GGA}[\rho_\sigma^{mBR}, \nabla\rho_\sigma^{mBR}]) \quad (28)$$

In eq 28, the exchange energy contribution $E_{X\sigma}^{LDA}$ due to the homogeneous electron gas, which is included in the GGA functional, completely vanishes by the subtraction in the parentheses. Furthermore, when $|\nabla\rho_\sigma|$ is equal to $|\nabla\rho_{X\sigma}^{mBR}|$ at a reference point, the exchange energy density $U_{X\sigma}^{mBR\text{-}GGA}$ is the same with $U_{X\sigma}^{mBR}$ at that point due to the cancellation of the gradient terms. It is worth noting that no empirical parameter is newly introduced in the construction of eq 28. For the SCF procedure to solve the Kohn−Sham equation, the functional derivative of eq 28 with respect to density ($\nu_{X\sigma}^{mBR\text{-}GGA}(\mathbf{r}) \equiv \delta E_{X\sigma}^{mBR\text{-}GGA}/\delta\rho_\sigma$) is necessary. We take essentially the same procedure as that proposed in the previous section, that is, the exchange potential $\tilde{v}_{X\sigma}^{mBR\text{-}GGA}(\mathbf{r})$ in Kohn−Sham equation is computed with the exponents α_0 and α_1 frozen. Then, these values are to be renewed after every SCF cycle to construct a new exchange potential. This process is iterated until the exponents as well as the electron density are converged.

2.4. Combination of Modified Becke−Roussel Model with LDA. The exchange functionals $E_{X\sigma}^{mBR}$ and $E_{X\sigma}^{mBR\text{-}GGA}$ discussed so far are along a unique line that starts from an inhomogeneous electron density as a prototypical hole distribution. However, these functionals have a crucial deficiency that they do not yield the exact LDA exchange energy at the homogeneous electron gas limit. This situation is also true for the original BR model described in section 2.1. Becke and Roussel proposed a method to recover the LDA exchange energy at the homogeneous limit by substituting $\gamma = 0.8$ in eq 9 instead of the true value of 1.0. Here, we take a mixing scheme (mBR-hyb) which hybridizes the $E_{X\sigma}^{mBR\text{-}GGA}$ with an LDA based exchange functional in a similar way to that proposed by Bahmann and Ernzerhof.[25] That is, we introduce the hybrid exchange functional $E_{X\sigma}^{mBR\text{-}hyb}$ as

$$E_{X\sigma}^{mBR\text{-}hyb} = \frac{1}{2}\left(\int d\mathbf{r}\, \exp(-cR^2)\rho_\sigma U_{X\sigma}^{LDA\text{-}GGA} + \int d\mathbf{r}\, (1 - \exp(-cR^2))\rho_\sigma U_{X\sigma}^{mBR\text{-}GGA}\right) \quad (29)$$

In eq 29, R is the distance between the reference point $\mathbf{r}$ and the center of the exchange hole described by the mBR model, and it is explicitly given by eq 20. $U_{X\sigma}^{LDA\text{-}GGA}$ denotes the standard LDA-based GGA exchange functional, and c expresses the mixing parameter. We note that, for the system with uniform electron density, $\rho_\sigma(\mathbf{r}) = \rho_\sigma^{max}$ holds wherever the reference point is chosen, and hence, R is equal to zero and the second term of the right-hand side of eq 29 vanishes. Thus, it is readily recognized that the functional of eq 29 recovers the exact exchange energy at the uniform gas limit. The mixing parameter c in eq 29 is, of course, an unknown parameter and considered to be an adjustable parameter to tune the distance at which the mBR exchange hole is mixing in. As noted in section 2.2, we at first take the parameter p in eq 19 as 2/3, and correspondingly the mixing parameter is chosen as $c = 1.0$ to ensure almost the exact value of 0.5 au for the electronic energy of a hydrogen atom. Then, the two-dimensional optimization for the parameter set (p, c) is carried out to attain the best performance of the present functional. It should be stressed that p and c are adjustable but surely contain physical meanings. Lastly, it should be noted that the GGA correction to the original BR model with the form of eq 1 can also be formulated in parallel to that for the mBR model described above.

3. Computational Details

Here, we present the computational details for the test calculations performed for small molecules. We have implemented the series of the mBR-based exchange functionals described above in our original code, which utilizes the real-space grids (RSG) and the pseudopotentials.[30−32] The methodological details for our RSG approach were presented in refs 23, 33, and 34. The kinetic energy operator in the one-electron Hamiltonian has been represented by the fourth-order finite-difference method. The nonperiodic hartree potential has been constructed by the method proposed in ref 35. The pseudopotentials derived by the method of Kleinmann and Bylander[36] have been used to express the effective potentials for valence electrons. A molecule of interest has been placed in the center of a cubic cell of which the axis has been uniformly discretized by 64 grids along each direction. The time-saving double grid approach proposed by Ono and Hirose[37] has been utilized to realize the rapid behavior of the nonlocal pseudopotentials as well as the pseudo-wave functions near the atomic cores. We have set the width of the original coarse grid at $h = 0.1518$ Å and that of the double grid at $h/3$. The convergence of the SCF procedure has been judged by the root-mean-square δ for the deviation of the electron density. To be specific, $\delta < 10^{-5}$ is imposed on the SCF convergence, which typically ensures the convergence within $10^{-6} \sim 10^{-7}$ E_h in the total electronic energy. The use of the pseudopotentials leads to an error due to its approximate construction. We have carefully checked the effects by comparing the atomization energies obtained by our code with those given by all-electron calculations with the Gaussian 03[38] program package. For these calculations, the PBE exchange has been used in combination with the Lee−Yang−Parr (LYP)[39] correlation functional. In the calculations by Gaussian 03, sufficiently large LCAO basis sets have been employed, where the quadruply split valence orbitals are used and polarization as well as diffuse atomic orbitals are augmented (aug-cc-pVQZ). Furthermore, the "Grid = UltraFine" option has been invoked to ensure the accuracy in the numerical integration of the DFT calculation.

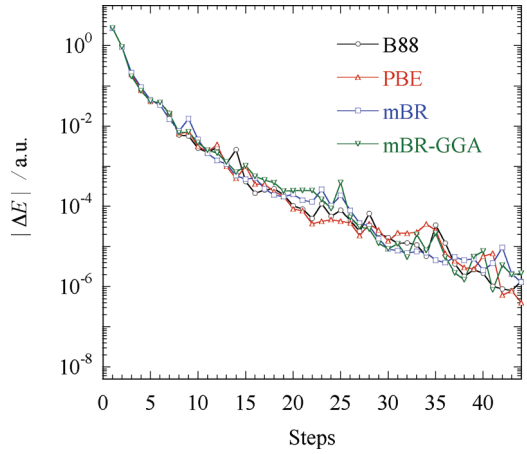

Figure 1. Convergence behaviors of the SCF procedures in KS-DFT that utilize the exchange functionals, B88, PBE, mBR, and mBR-GGA. Absolute values of the energy differences between neighboring steps are plotted against the SCF steps.

4. Applications and Tests

In this section, we present the results of the numerical applications of the mBR-based functionals and compare them with the conventional GGA functionals. In section 4.1, the convergence behaviors in the SCF procedures for these functionals are examined. In sections 4.2 and 4.3, the enhancement factors as well as the exchange energy densities and the exchange potentials have been plotted as functions of the position of the reference electron placed in a molecular system. In section 4.4, we present the results of the atomization energies, ionization potentials, proton affinities, and enthalpies of formation to discuss the accuracy and efficiency of the present approach. The exchange-hole functions given by this model for several reference points in a molecule are plotted in section 4.5 to make comparisons with LDA and the exact exchange holes. Hereafter, we refer to the exchange functionals defined by eqs 22, 28, and 29 by the shorthand notations mBR, mBR-GGA, and mBR-hyb, respectively.

4.1. Convergence Behavior. As described in section 2.2, the exchange energy functional $E_{X\sigma}^{mBR}$ of eq 22 includes density-dependent parameters (α, R) which are iteratively determined in the SCF procedure as well as the electron density. This possibly leads to a numerical instability in the SCF convergence to a certain extent. To see this in detail, we have examined the convergence rate in SCF for the mBR and mBR-GGA exchange functionals which are, respectively, given in the forms of eqs 22 and 28. The PBE exchange functional has been used for the GGA correction term $E_{X\sigma}^{GGA}$ in eq 28. We have also investigated the convergence behaviors of the SCF calculations with B88 and PBE exchange functionals to make comparisons. A water molecule has been used for these test calculations, where the wave functions have been updated by the scaled steepest descent (SD) algorithm starting from the same initial guess. The geometry of the water has been taken from ref 40.

In Figure 1, the log plots have been shown for the absolutes of the differences in the electronic energies between adjacent steps in the SCF procedure against the SCF step number. It is clearly shown that the convergence rates of the SCF calculations with mBR or mBR-GGA are comparable to those with the conventional GGA functionals such as B88 or PBE. Thus, it has been demonstrated that no serious numerical instability takes place in the SCF procedures for the practical applications of the series of the mBR exchange functional. We remind the reader that the pseudopotentials have been used through these test calculations, and they may possibly support the stability in the convergence. Unfortunately, we could not check the effect of the use of pseudopotentials since an LCAO-based program package equipped with our approach is not available.

4.2. Enhancement Factor. To investigate the property of an exchange functional mBR, we have evaluated the exchange enhancement factor $F_{X\sigma}^{mBR}$ defined by

$$E_{X\sigma}^{mBR} = \frac{1}{2}\int d\mathbf{r}\, \rho_\sigma \cdot U_{X\sigma}^{LDA} \cdot F_{X\sigma}^{mBR} \tag{30}$$

In eq 30, $U_{X\sigma}^{LDA}$ is the exchange energy density of the uniform electron gas derived by Dirac[1] and is given by

$$U_{X\sigma}^{LDA} = -3\left(\frac{3}{4\pi}\right)^{1/3}\rho_\sigma^{1/3} \tag{31}$$

Equations 22 and 30 suggest that the factor $F_{X\sigma}^{mBR}$ represents the ratio of the exchange energy density $U_{X\sigma}^{mBR}$ given in eq 21 with respect to $U_{X\sigma}^{LDA}$. We have performed the same evaluations for the functionals mBR-GGA and mBR-hyb. Usually, the enhancement factor for a GGA functional is plotted as a function of the dimensionless parameter $x_\sigma \equiv |\nabla\rho_\sigma|/\rho_\sigma^{4/3}$, which represents the inhomogeneity of the electron density since a usual GGA functional depends only on x_σ. However, our functional is also dependent on the maximum value of the electron density as well as the eigenvalue of the HOMO besides the gradient of the density. Therefore, we have computed $F_{x\sigma}$ for a real system with a closed shell electronic structure. Specifically, we have chosen a water molecule as a model system; then, the enhancement factors have been plotted by varying the position of the reference electron along the symmetry axis of the water molecule. For the calculations of the enhancement factors for each functional shown below, we have adopted the electron density obtained by using the B88 functional without correlation.

In Figure 2, we have plotted the enhancement factors for the functionals, mBR, mBR-GGA, and mBR-hyb. The PBE functional has been employed for the GGA correction in the mBR-GGA and mBR-hyb functionals. The factors for the functionals B88 and PBE have also been depicted in the figure to make comparisons. The inhomogeneity parameter x_σ has been superimposed in Figure 2. The horizontal axis of Figure 2 represents the coordinate of the reference electron placed on the symmetry axis of the water molecule for which an experimental geometry[40] has been used. The origin of the axis has been placed on the oxygen atom of the water. In addition, the center of molecular mass has been adjusted to the negative direction of the axis.

At first, we made comparisons between the behaviors of $F_{x\sigma}$ for the conventional GGA exchange functionals B88 and PBE. These two functionals start from the same basis;

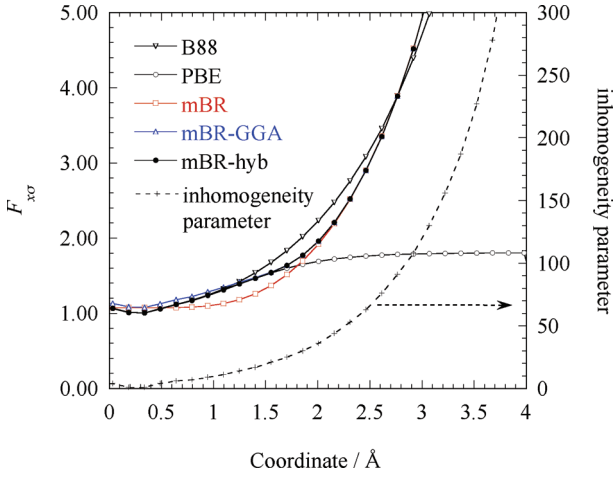

Figure 2. Plots for the enhancement factors given by B88, PBE, mBR, mBR-GGA, and mBR-hyb functionals. The horizontal axis represents the position of the reference electron placed on the symmetry axis of a water molecule. The oxygen atom is taken as the origin of the axis. The electron density obtained by the KS-DFT calculation using the B88 functional without correlation is employed to evaluate the enhancement factors with these functionals. The dimensionless parameter x_σ is also drawn in the figure.

nevertheless, $F_{x\sigma}$ for B88 shows a distinct deviation from that for PBE. We observe in Figure 2 the enhancement factor $F_{X\sigma}^{B88}$ for the B88 functional increases rapidly as the reference electron moves away from the molecule, and this behavior agrees with that of the inhomogeneity parameter x_σ. In contrast to B88, the enhancement factor $F_{X\sigma}^{PBE}$ for PBE increases modestly and converges to a certain value as r increases. Such a discrepancy in the region of large inhomogeneity can be attributed to the difference in the physical constraints that are imposed on these functionals. Both the B88 and the PBE exchange functionals originate from basically the same analytic function with a nondivergent property for the increase of x_σ.[9,41] On the basis of this function, the B88 functional was constructed so that it recovers the $-1/r$ asymptotic behavior of the exchange energy density,[8] while the PBE functional was subjected to the constraint of the local Lieb−Oxford bound.[42] Consequently, the enhancement factor for B88 increases rapidly in the asymptotic region, and that for PBE converges to 1.804 at the limit of the large inhomogeneity, as shown in Figure 2. Later, Zhang and Yang proposed a method termed revPBE by choosing the asymptotic value of $F_{X\sigma}^{PBE}$ as 2.245 instead of 1.804.[43] This modification can be validated by the fact that the adoption of the Lieb−Oxford bound for all positions of the reference electron is just a sufficient but not necessary condition to satisfy the integrated Lieb−Oxford bound. Anyway, we observe that the enhancement factors for B88 and PBE functionals coincide well in the region of small x_σ, and they diverge rapidly as the reference electron moves away from the molecule. From a numerical point of view, we note that such a divergence does not have serious effects on the energetics because the region of large inhomogeneity coincides with the small density tail, and therefore with exponentially small energy density owing to the $\rho^{1/3}$ term from the LDA part.

The enhancement factor $F_{X\sigma}^{mBR}$ for the functional mBR shows the correct asymptotic behavior similar to the B88 functional by virtue of the fact that the atomic electron density is adopted as a model exchange hole. Here, it should be emphasized that such an important property is built-in in the model and is naturally simulated without making a special device for it. In Figure 2, it can also be recognized that the factor $F_{X\sigma}^{mBR}$ is almost comparable to $F_{X\sigma}^{LDA}$ from the short to middle range of the reference position (note that $F_{X\sigma}^{LDA} = 1$ holds everywhere by the definition of eq 30). Thus, the deviation of the mBR functional from B88 or PBE has been found to be serious for the reference electron placed on the coordinate of ∼1.5 Å. The enhancement factor $F_{X\sigma}^{mBR\text{-}GGA}$ for eq 28 shows that this unpleasant situation can be substantially alleviated by the GGA correction adopted in the mBR functional.

As for the short-range behaviors of $F_{X\sigma}^{mBR}$ and $F_{X\sigma}^{mBR\text{-}GGA}$, it is shown in Figure 2 that they slightly overestimate those of the LDA-based exchange functionals. According to the prescription by Perdew et al.,[16] an exchange functional should reproduce Dirac's exact exchange at the uniform electron gas limit. The functional mBR-hyb given by eq 29 is designed so that it recovers the LDA exchange energy at the uniform gas limit. Consequently, the enhancement factor $F_{X\sigma}^{mBR\text{-}hyb}$ realizes the sound behavior in the region of the small inhomogeneity. Thus, the mBR-hyb functional has a desirable property in the enhancement factor from the short- to long-range region of the reference electron.

4.3. Exchange Energy Density and Exchange Potential. One of the important features of the mBR-model based approach lies in the possibility that it can recover the correct long-range behaviors of the exchange energy density $U_{x\sigma}$ and the exchange potential $v_{x\sigma}$. $U_{x\sigma}$ represents the exchange energy per electron felt at a given position and is explicitly defined by an equation parallel to eq 3. It can be readily verified that exact $U_{x\sigma}$ behaves as $-1/r$ in the asymptotic region of $r\rightarrow\infty$ (r is roughly the distance between the reference point and the molecule of interest). The exchange potential $v_{x\sigma}$ given by the functional derivative of exchange energy $E_{x\sigma}$ with respect to density (parallel to eq 23) is also known to decay asymptotically in the Coulombic manner as $-1/r$. In the following, we have investigated the behaviors of $U_{x\sigma}$ and $v_{x\sigma}$ obtained with the exchange functional mBR-hyb and compared it with conventional GGA functionals. For these calculations, we have employed the same system used in the calculation of the enhancement factors presented in section 4.2.

In Figure 3, the exchange energy density for the mBR-hyb functional has been plotted for the variation of the position of the reference point. Those for the B88 and the PBE functionals have also been drawn in the figure. The horizontal axis is the coordinate of the reference electron of which the origin has been taken in the same manner as in section 4.2. For the construction of the Coulomb potential $-1/r$ in the figure, the origin has been set at the nuclear-charge weighted center of mass. Explicitly, a coordinate of −0.118 Å is chosen as the origin of the Coulomb potential. We observe in Figure 3 that the exchange energy density for B88 functional

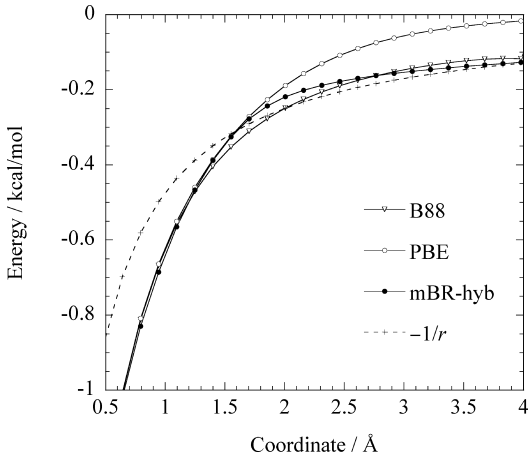

Figure 3. Plots for the exchange energy densities given by B88, PBE, and mBR-hyb functionals. The definition of the horizontal axis is the same as in Figure 2. The electron density used in the construction of Figure 2 is employed for these calculations.

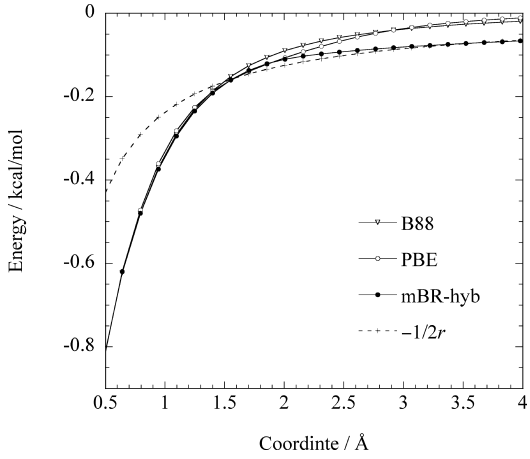

Figure 4. Plots for the exchange potentials given by B88, PBE, and mBR-hyb functionals. The definition of the horizontal axis is the same as in Figure 2. The same electron density used in the construction of Figure 2 is employed for these calculations.

asymptotically behaves as $-1/r$, while that for PBE decays rapidly as the reference electron moves away from the molecule. The origin of such a difference between these two GGA functionals is the same as that of the deviation in the enhancement factors discussed in section 4.2. That is, the bifurcation of the exchange energy densities arises from the difference in the constraints imposed on the functionals. In accord with the B88 fucntional, the curve for mBR-hyb also shows correct asymptotic behavior by virtue of the exchange hole based on the mBR model. We again emphasize that the long-range nature of the exchange energy density is naturally incorporated in the mBR model since it mimics the hole in a hydrogenic atom.

In Figure 4, it is shown that the exchange potential v_x for B88 decays rapidly in contrast to the behavior of the exchange energy density in the long range. This asymptotic behavior coincides with that of the PBE functional. Such an undesirable behavior of the exchange potential of the B88 functional was analyzed in ref 44, and it was proved analytically that any exchange functional $E_{x\sigma}$ with the form of

$$E_{X\sigma}[\rho_\sigma] = \int \rho_\sigma^{4/3} f(x_\sigma)\, d\mathbf{r} \tag{32}$$

does not satisfy the $-1/r$ asymptotic relation when $f(x)$ in eq 32 is constructed so that the exchange energy density behaves asymptotically as $-1/r$. Specifically, v_x for the B88 functional decays non-Coulombically as k/r^2 with a negative constant k. In contrast to B88 and PBE, we observe that the potential for the mBR-hyb functional decays Coulombically in the asymptotic region; however, it recovers only half of the $-1/r$. The $-1/2r$ asymptotic behavior of the mBR-based approach is readily understood by consulting eq 23. In the region of the small electron density, it is verified that the exchange potential $v_{x\sigma}$ is dominated by half of the exchange energy density $U_{x\sigma}$ which behaves as $-1/r$. Thus, it has been demonstrated that the exchange potential of the functional based on the mBR exhibits Coulombic asymptotic behavior of $-1/2r$.

Table 1. Mean Absolute Deviations of Atomization Energies for 35 Molecules in the G2 Set Evaluated by LDA, mBR, mBR-PBE, mBR-hyb, and PBE Exchange Functionals[a]

	LDA	mBR	mBR-PBE	mBR-hyb	PBE
mean abs. deviation	38.5	32.2	16.4	7.9	7.7

[a] Deviations are in the units of kcal mol^{-1}. The LDA exchange is combined with the local correlation term given by Perdew and Zunger.[12] The rest of the functionals are used along with the LYP functional.[39] In the mBR-hyb calculation, the parameters p and c in eqs 19 and 29 are those not optimized (p = 2/3 (0.667), c = 1.0). We refer the readers to Supplementary Table 1 in the Supporting Information for the values of individual molecules.

Table 2. Mean Absolute Deviations of Ionization Potentials for 13 Molecules in the G1 Set Evaluated by LDA, mBR-hyb, and PBE Exchange Functionals[a]

	LDA	mBR-hyb	PBE
mean abs. deviation	0.3	0.2	0.2

[a] Deviations are in the units of eV. The correlation functionals used are common to those in Table 1. In the mBR-hyb calculation, the parameters p and c in eqs 19 and 29 are those not optimized (p = 2/3 (0.667), c = 1.0). We refer the readers to Supplementary Table 2 in the Supporting Information for the values of individual molecules.

4.4. Properties of Small Molecules. In this section, we have assessed the performance of the series of the mBR-based exchange functionals by computing atomization energies, ionization potentials, and proton affinities respectively for 35, 13, and 3 molecules supplied in the G1 and G2 molecular sets.[45,46] The method to determine the asymptotic value of the exponent α_0 of the exchange hole through eqs 17 and 18 necessitates the eigenvalue ϵ_{HOMO} of HOMO to be negative. Unfortunately, ϵ_{HOMO} for anionic molecules are positive in most cases, and hence, the performance check for the electron affinities could not been done. In this sense, our approach lacks robustness and needs to be refined in the procedure to determine the exponent α_0. In Tables 1, 2, 4, and 5, we have only presented the statistics for each property.

Table 3. Proton Affinities for Three Molecules in the G1 Set Evaluated by LDA, mBR-hyb, and PBE Exchange Functionals[a]

system	LDA	mBR-hyb	PBE	expt.
NH_{32}	206.5	210.2	207.1	211.2
$H_{32}O$	167.4	170.7	167.3	173.5
C_2H_2	153.6	158.9	154.9	155.7

[a] Energies are in the units of kcal mol^{-1}. The correlation functionals used are common with those in Table 1. In the mBR-hyb calculation, the used parameters p and c in eqs 19 and 29 are those not optimized (p = 2/3 (0.667), c = 1.0). The experimental values are taken from ref 45, from which the ZPEs are removed. ZPEs are obtained by the same manner as in Table 1.

Table 4. Atomization Energies for 35 Molecules in the G2 Set Evaluated by mBR-hyb, the Original BR Functional, and That Hybridized with the Hartree−Fock (HF) Exchange[a]

	mBR-hyb	BR	BR+HF
mean abs. deviation	4.9	4.3	1.6

[a] Energies are in the units of kcal mol^{-1}. The mBR-hyb exchange functional is used along with LYP correlation functional,[39] while original BR and BR+HF functional are combined with the correlation energy of ref 48. In the mBR-hyb calculation, the parameters p and c in eqs 19 and 29 are those optimized (p = 0.7/3 (0.233), c = 0.15). We refer the readers to Supplementary Table 3 in the Supporting Information for the values of individual molecules.

Table 5. Mean Absolute Deviations of Enthalpies of Formations for 63 Molecules in the G3 Set Evaluated by mBR-hyb and the PBE Exchange Functional[a]

	mBR-hyb	PBE
mean abs. deviation	9.4	18.7

[a] Deviations are in the units of kcal mol^{-1}. The correlation functionals used are common to those in Table 1. In the mBR-hyb calculation, the parameters p and c in eqs 19 and 29 are those optimized (p = 0.7/3 (0.233), c = 0.15). We refer the readers to Supplementary Table 4 in the Supporting Information for the values of individual molecules.

We have supplied "supporting information" for the references to the results for individual molecules.

We have computed the atomization energies by using mBR, mBR-GGA, and mBR-hyb functionals and compared them with experimental values in Table 1. The results by the LDA and PBE functionals have also been provided in the table for comparisons. All exchange functionals except for LDA have been used in combination with the LYP correlation functional.[39] In the LDA calculation, on the other hand, the local correlation functional proposed by Perdew and Zunger (PZ)[12] has been used. Hereafter, we omit the notation of "LYP" or "PZ" specifying the correlation functional for the sake of brevity. Mean absolute deviation (MAD) of the atomization energies from the experimental values has been computed for each functional. As described in the Computational Details, we have checked the error due to the pseudopotentials utilized in the real-space grids scheme by performing all-electron calculations with Gaussian 03 with a sufficiently large basis set (aug-cc-pVQZ). The MAD of the PBE functional derived by Gaussian 03 has been estimated to be 8.2 kcal/mol, which shows good agreement with the value of 7.7 kcal/mol given by our code. It may be reasonable to conclude that the use of the pseudopotential does not seriously affect the energetics at least for these molecules. The MAD for the mBR calculation has been obtained as 32.2 kcal/mol, and it has been found that the mBR approach gives rather better results than the LDA level calculations. However, it is quantitatively far from satisfaction to predict the energetics for the chemical reactions. It has been found that the introduction of the GGA correction to the mBR functional (mBR-GGA) significantly improves the computational accuracies in the atomization energies. The value of MAD has been reduced to 16.4 kcal/mol. It should be noted that the MAD given by mBR-GGA lies in the middle of those given by two sorts of calculations based on the *original* BR approach conducted by Neumann et al.[21] To be specific, they performed calculations by setting the values of γ in eq 4 at $\sim$1 and 0.8. Then, the MAD values were given as 10.3 and 21.1 kcal/mol for the calculations of γ = 1.0 and 0.8, respectively. As described in section 2.4, the relation of γ = 1.0 holds in the exact expression of the spherically averaged Taylor expansion of the exchange hole, while the choice of γ = 0.8 is intended to recover the exchange energy at the homogeneous electron gas limit. We conclude that the mBR-GGA level funtional is almost comparable to the original BR approach in the computational accuracy for the atomization energy. However, it is obvious that the mBR-GGA functional is still less accurate than the PBE functional. We can see in the table that further improvement can be achieved by combining the mBR-GGA with the LDA-based functional (mBR-hyb). The hybridization with the LDA functional reduces the MAD value from 16.4 to 7.9 kcal/mol. Thus, the realization of exchange energy for the uniform electron gas limit at low x_σ is crucial to ensuring the computational accuracy of the functional as suggested in ref 16. Thus, it has been revealed that mBR-hyb is comparable to the PBE functional.

By utilizing the mBR-hyb functional we have also computed the ionization potentials and proton affinities for some molecular systems, the results of which are, respectively, presented in Tables 2 and 3. And comparisons have been made with the results given by LDA and PBE. We can see that the MAD for mBR-hyb is comparable to that for PBE in the calculations of the ionization potentials. As for the proton affinity, the mBR-hyb functional shows slightly better results than PBE, though the number of the samples is very small.

Here, we emphasize that there is still room for further refinement in the mBR-hyb functional. The adjustable parameter p in eq 19 has so far been taken as 2/3, which is simply the maximum of the allowed value which ensures the existence of the real value of r defined by eq 20. In addition, the mixing parameter c in eq 29 has been chosen somewhat arbitrarily as 1.0 to reproduce the exact electronic energy of hydrogen. To optimize these parameters, we have extended the benchmark molecules to the G3 set.[47] Explicitly, 63 molecules in the G3 set have newly been added to the above 35 molecules (98 molecules in total) for the two-parameter fit to the experimental atomization energies and the enthalpies of formation. Molecules in the G3 set that

include the S atom have been excluded from the benchmark test because the pseudopotential for the S atom is not available in the present version of our program. To be specific for molecules in the G3 set that include relatively large hydrocarbons, we have prepared 90 grid points along each direction of the real-space cell to ensure that the wave functions will be enclosed within the cell. This optimization has led to a set of values $p = 0.7/3$ (0.233) and $c = 0.15$. The atomization energies for the above 35 molecules computed by using the parameters have been presented in Table 4 in comparison with the experimental values. It has been demonstrated that MAD has been successfully decreased to 4.9 from 7.9 kcal/mol for the 35 molecules in the G2 set. In the second and third columns in Table 4, we have also presented the results[24] obtained by Becke, who utilized the original Becke−Roussel approach. It should be noted, however, that the computations were performed using the orbitals and densities given at the outset by LDA calculations. The second column shows the results by the BR exchange functional in an unaltered form ($\gamma = 1.0$ in eq 4) in combination with the correlation energy based on the inhomogeneous electron gas model,[48] which gives the MAD from experiment as 4.3 kcal/mol. Thus, it has been found that the parameter-optimized mBR-hyb functional is almost comparable in accuracy to the original BR functional. The data in the third column were obtained by replacing the small fraction of the exchange term by the exact (Hartree−Fock) exchange with mixing parameter $c_X = 0.154$. By mixing the exact exchange in the functional, the MAD value greatly decreased to 1.6 kcal/mol. As described in section 2.2, the size consistency is violated in the present method. We have checked the energy deviation due to the size inconsistency by dissociating the O−H bond in a H_2O molecule. The absolute energy of the sufficiently separated OH and H complex subtracted by the sum of the energies of the constituent fragments has been evaluated as 1.7 kcal/mol. The O−H bond energy has been obtained as 125.0 kcal/mol, and hence, the size inconsistency is not so serious in this case. However, we note that care must be taken for this shortcoming in the functional.

As for the molecules in G3 set, we have computed the enthalpies of formation with the procedure described in the G2 and G3 papers. The enthalpy of formation $\Delta H_f'(A_xB_y)$ at 298 K for a compound such as A_xB_y can be expressed as

$$\Delta H'_f(A_xB_y) = \Delta H_f(A_xB_y) + \{H'(A_xB_y) - H(A_xB_y)\} - x\{H'(A) - H(A)\}_{st} - y\{H'(B) - H(B)\}_{st} \quad (33)$$

where ΔH_f denotes the enthalpy of formation at 0 K, and H' and H stand for the enthalpies at 298 and 0 K, respectively. The corrections for enthalpies of elements are for the standard states of elements and denoted by "st" in eq 33. $\Delta H_f(A_xB_y)$ in eq 33 can be, further, decomposed into

$$\Delta H_f(A_xB_y) = H(A_xB_y) - xH(A) - yH(B) + x\Delta H_f(A) + y\Delta H_f(B). \quad (34)$$

The first three terms in the right-hand side of eq 34 constitute the minus atomization energy corrected by zero-point vibrational energy (ZPE). In the calculation of eqs 33 and 34, the experimental values have been adopted by the elemental enthalpies of formation and by their corrections.[49] Furthermore, it has been assumed that the corrections for the enthalpies of compounds as well as ZPE can be estimated with substantial accuracies by the G3 theory.[50] Then, the errors in the theoretical enthalpies of formation can be reasonably ascribed to those in the atomization energies. In the first column in Table 5, we have presented the enthalpies of formation computed by the mBR-hyb functional with the optimized parameters $(p, c) = (0.233, 0.15)$. The MAD for the 63 molecules in the G3 set has been obtained as 9.4 kcal/mol, where the *n*-octane (C_8H_{18}) molecule has given the maximum absolute error of 23.3 kcal/mol. It should be noted that absolute errors in enthalpies of formation increase with molecular size because of the increase in the atomization energies. For instance, the atomization energy of *n*-octane has been evaluated as 2451 kcal/mol. The third column of Table 5 shows the results given by the Gaussian package using the PBELYP functional with the aug-cc-pVQZ basis set, where the MAD value has been obtained as 18.7 kcal/mol and the maximum absolute error has been obtained as 40.6 kcal/mol for pyrimidine ($C_4H_4N_2$). Furthermore, we have also evaluated the enthalpies of formation by using PBE exchange combined with the PBE correlation functional using the same basis set, which have led to a MAD value of 22.0 kcal/mol. Thus, it has been demonstrated that the mBR-hyb functional with the optimized parameters is superior to a conventional GGA functional for the evaluation of atomization energies of this molecular set.

Last, we present in Figure 5 the results for the computation of the hydrogen-bond (HB) energy curve of a water dimer as a function of the distance between oxygen atoms. The illustration for the geometry of the water dimer has also been drawn in Figure 5. The geometrical parameters of the constituent water molecules have been fixed at those of the TIP4P model ($r_{OH} = 0.9572$ Å, HOH = 104.52°)[51] for the variation of the O−O distance. To construct a reliable standard for the HB energy curve, we have performed a CCSD(T)[52]/aug-cc-pVTZ calculation with the counterpoise corrections by utilizing the Gaussian 03 package. To make comparisons, the computations by the LDA and the PBE functionals have also been carried out by Gaussian 03 in the same manner as the CCSD(T) calculation. In the mBR-hyb calculations, we have employed both parameters that were optimized ($p = 0.7/3$ (0.233), $c = 0.15$) and not optimized ($p = 2/3$ (0.667), $c = 1.0$). In the real-space cell, 90 grids have been placed along each axis with interval $h = 0.118$ Å, and the width of the dense grid has been set at $h/10$. In accord with the findings of a previous work,[53] we observe in Figure 5 that the LDA functional seriously overestimates the binding energy and underestimates the optimum O−O distance. However, the behavior of the HB energy curve is dramatically improved by the introduction of the GGA correction, as exhibited in the PBE curve, which shows comparable behavior with the CCSD(T) result. And, the curve for mBR-hyb with unoptimized parameters lies between those for CCSD(T) and PBE. Importantly, the mBR-hyb curve also shows good agreement with CCSD(T) after the parameter optimizations. Thus, it is demonstrated that

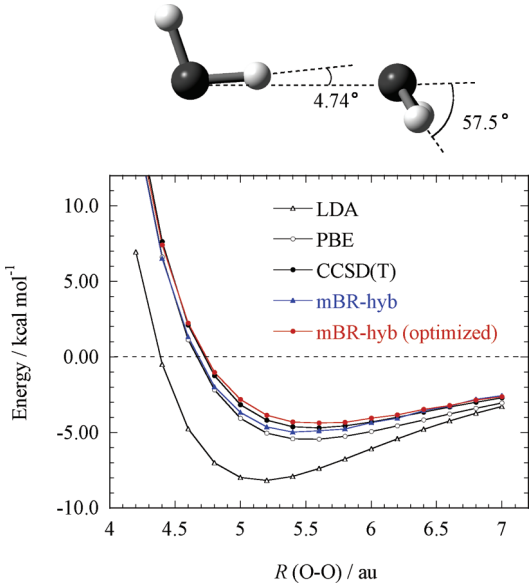

Figure 5. Potential energy curves of a hydrogen bond of a water dimer computed by CCSD(T), LDA, PBE, and mBR-hyb calculations. In the mBR-hyb calculations, both optimized (p = 0.7/3 (0.233), c = 0.15) and nonoptimized parameters (p = 2/3 (0.667), c = 1.0) are used. The horizontal axis represents the O−O distance. The notation of LDA stands for the calculation of Dirac's exchange in combination with the correlation functional proposed by Perdew and Zunger. In the PBE and the mBR-hyb calculations, the correlation energies are estimated by the LYP functional.

the mBR-hyb functional also gives a satisfying result in the computation of the HB energy.

From these test calculations so far, we conclude that the mBR-hyb functional offers energetics with comparable or yet superior accuracy as compared to a sophisticated GGA functional based on the LDA. This greatly encourages further improvements on the mBR-based functionals for practical applications to atoms or molecules.

4.5. Exchange-Hole Function. In this section, we have plotted the exchange-hole distribution of the present approach in comparison with that of LDA and the exact one. We first make a formulation for the exact exchange hole. The exact exchange hole $\rho_{X\sigma}(\mathbf{r}, \mathbf{r}')$ is defined by

$$\rho_{X\sigma}(\mathbf{r}, \mathbf{r}') = \frac{|\rho_{1\sigma}(\mathbf{r}, \mathbf{r}')|^2}{\rho_\sigma(\mathbf{r})} \tag{35}$$

where $\rho_{1\sigma}(\mathbf{r}, \mathbf{r}')$ is the one-body density matrix for spin σ and is simply expressed in terms of the one-electron wave functions; thus,

$$\rho_{1\sigma}(\mathbf{r}, \mathbf{r}') = \sum_i^{\text{occ}} \phi_{i\sigma}(\mathbf{r})\, \phi_{i\sigma}^*(\mathbf{r}') \tag{36}$$

The spherically averaged exchange-hole function $\rho_{X\sigma}^{SA}(\mathbf{r},s)$ can be written as

$$\rho_{X\sigma}^{SA}(\mathbf{r}, s) = \frac{1}{4\pi s^2} \int_{\Omega_s} \rho_{X\sigma}(\mathbf{r}, \mathbf{r} + \mathbf{s})\, d\mathbf{s} \tag{37}$$

where Ω_s denotes the integration over a sphere of radius s centered at a reference point $\mathbf{r}$. On the other hand, the exchange hole based on the mBR model is represented by eq 12, and its spherical average $\rho_{X\sigma}^{SA\text{-}mBR}(\alpha,R;s)$ is obtained by simple algebraic manipulations; thus,

$$\rho_{X\sigma}^{SA\text{-}mBR}(\alpha, R;s) = \frac{\alpha^{1/2}}{4\pi^{3/2}Rs}(\exp\{-\alpha(R - s)^2\} - \exp\{-\alpha(R + s)^2\}) \tag{38}$$

It is useful to note that eq 38 corresponds to eq 17 of ref 18 that utilizes the Slater-type function as an exchange-hole model. We also note that (α, R) in eq 38 has been determined from the spin density $\rho_\sigma(\mathbf{r})$ as described in section 2.2 where the scaling parameter p in eq 19 has been set at 0.233. In the LDA approach, the exchange hole is spherically symmetric around $\mathbf{r}$ and is given by

$$\rho_{X\sigma}^{SA\text{-}LDA}(\mathbf{r}, s) = 9\rho_\sigma(\mathbf{r})\left(\frac{\sin t - t\cos t}{t^3}\right)^2 \tag{39}$$

where

$$t = (6\pi^2\rho_\sigma(\mathbf{r}))^{1/3}s \tag{40}$$

We have plotted the exchange-hole distributions expressed by eqs 38, 39, and 40 for various positions of the reference electron in a molecule to make comparisons. Furthermore, we have also performed calculations with the mBR functional, where the parameters (α, R) in eq 38 have been determined by the procedure proposed in the original Becke−Roussel approach. Explicitly, (α, R) are obtained by imposing the conditions that zeroth- and second-order terms in the Taylor expansion of eq 4 coincide with those of the exchange-hole model defined by eq 12. The computational procedure for the Gaussian-type function is parallel to that for the Slater-type one. In the following, we term this approach the original mBR.

For the construction of the exchange hole, we have employed a water molecule with the same geometry that was used in section 4.2. In the real-space grid approach, 90 grids have been placed along each axis with grid spacing h = 0.0679 Å, and the width of the dense grids has been set at h/5. We have constructed the exchange-hole functions by using the same spin density and one-electron wave functions obtained from the outset by the B88 exchange functional without electron correlations. In Figure 6a−c, we have compared the behaviors of exchange-hole functions for three different positions of the reference electron. In Figure 6a, the reference point has been placed at the oxygen atom. It appears in the contour map that the exchange-hole function is dominated by the $2a_1$ orbital of the water molecule. The exchange-hole functions for mBR and LDA show good agreement with the exact one, while the original mBR model slightly deviates from the others. Anyway, it has been demonstrated that these three approaches can properly simulate the behavior of the exact exchange hole. In Figure 6b, the reference point has been placed below the oxygen atom along the symmetry axis of the molecule. In this case, we recognize that the exchange hole distribution is character-

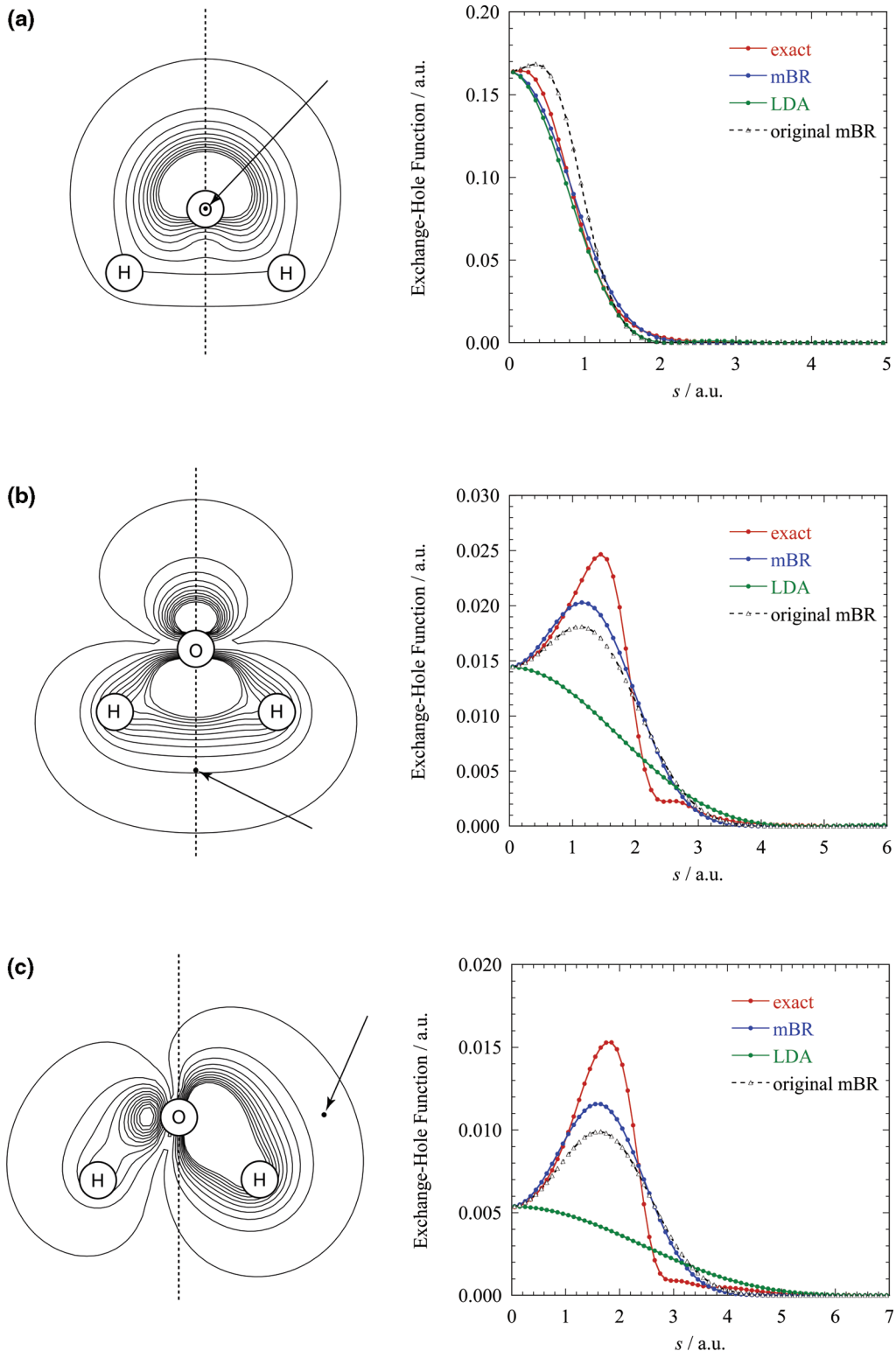

Figure 6. Contour plots of the exchange-hole functions for the reference electron placed at various positions on the molecular plane of H_2O (left). Spherically averaged exchange holes as functions of the distance *s* from the reference point (right). Arrows in the contour map indicate the positions of the reference electrons. The value of the outermost contour line is 0.001 au, and the interval is set at 0.01 au.

ized by the $3a_1$ orbital. It is shown in the plot that the LDA approach fails to reproduce even the qualitative behavior of the exact exchange hole. This originates from the fact that the maximum peak of the exchange hole always locates at the reference point in the homogeneous electron gas. On the other hand, we observe that the mBR approach successfully simulates the behavior of the exact exchange hole, though the detailed structures of the hole cannot be reproduced. This directly demonstrates the advantage of the mBR approach that it allows the exchange hole being attached at the molecule even when the reference electron is moved far apart from the system. We have also plotted the exchange

hole function given by the original Becke-Roussel procedure. The peak position as well as the overall behavior of the original mBR shows good agreement with those of the mBR exchange hole. In Figure 6c, the position of the reference electron has been chosen so that the exchange hole is characterized by the $1b_2$ orbital. Again, we see that the mBR approach can illustrate the appearance of the exact exchange-hole distribution in contrast to LDA. The mBR approach also shows excellent agreement with the original mBR.

5. Summary and Conclusions

The point of the BR approach is to mimic the exchange hole function at a given reference point by an electron distribution of a hydrogenic atom. This allows the exchange hole to be attached to the molecule even when the reference electron is placed far apart from the system, in contrast to the LDA approach, which naturally improves the asymptotic behavior of the exchange energy density. In this paper, we have proposed a series of exchange functionals based on the mBR model for the purpose of finding a new route to the exchange functional. Our approach to the simple realization of the mBR-based functional consists of three steps. The first step is to determine the parameters (α, R) that specify the distribution of the mBR exchange hole with respect to the reference point. The width α of the hole is to be obtained from its asymptotic values α_1 and α_0 through eq 19. Then, the distance r between the reference point and the exchange hole is readily computed from the constraint that the depth of the hole is equal to the spin density at the reference point. In the second step, we make a GGA correction to the functional obtained in the first step (mBR-GGA). More specifically, as expressed in eq 28, the conventional GGA formula has been adopted to take into account the gradients of the spin density as well as the mBR exchange hole. Third, the gradient-corrected mBR functional thus obtained is combined with the LDA approach as in the form of eq 29 to reproduce the exchange energy at the homogeneous electron gas limit (mBR-hyb).

We have examined the behaviors of the enhancement factors of the mBR-based exchange functionals with respect to the distance between the reference electron and a molecular system. It has been demonstrated that the mBR-hyb functional shows an excellent overall behavior in accord with B88. The exchange energy densities of the mBR-based approaches have shown correct asymptotic behaviors of $-1/r$ by virtue of the fact the electron density of a hydrogenic atom is taken as a model of the exchange hole. Further, the exchange potential in mBR-hyb has also been shown to decay Coulombically in contrast to B88 and PBE; however, it recovers only half of the $-1/r$ potential in the asymptotic region. We have assessed the performance of the series of the mBR exchange functionals combined with the LYP correlation functional by computing several properties of the small molecules in the G1, G2, and G3 sets. It has been found that the computational accuracy for atomization energies can be systematically improved by the three steps noted above. It has been demonstrated that the mBR-hyb functional is almost comparable in accuracy to the GGA functional of PBE. Optimization of only two adjustable parameters in mBR-hyb functional has shown to provide much better results in the atomization energies and enthalpies of formation. The MAD value for the atomization energies of 35 molecules in the G2 set has been evaluated as 4.9 kcal/mol by the mBR-hyb functional with optimized parameters. And the MAD for the enthalpies of formations of 65 molecules in the G3 set has been computed as 9.4 kcal/mol. The calculations for the water dimer have revealed that the mBR-hyb is adequate enough to reproduce rather weak interactions such as hydrogen bonds.

The results of the test calculations obtained so far is very encouraging for further improvement of the mBR-based functional. In spite of the success, the present method clearly has deficiencies in some respects. First of all, the procedure to determine the exponent α_0, that utilizes the energy level of the HOMO, must be refined for the applications to anionic systems. The use of the orbital energy also leads to an undesirable property in the functional, that is, the lack of size consistency. Second, the parameters p and c which appear, respectively, in eqs 19 and 29 should be optimized for molecular systems involving all electrons to avoid the influence of the pseudopotentials used in the present calculations. We conclude that the route to develop the exchange energy functional that begins from the BR model is worth consideration as a potential candidate for the establishment of the exchange functional suitable for the applications to atoms or molecules.

Acknowledgment. This work is supported by a Grant-in-Aid for Scientific Research on Priority Areas (Nos. 18031022 and 21118512) from the Ministry of Education, Science, Sports and Culture of Japan. H.T. would like to thank K. Kubota and K. Maruyama for their help in preparing the data in Tables 1∼5. H.T. is also grateful to Prof. N. Matubayasi in Kyoto university for his continuous encouragement of this work.

Supporting Information Available: Additional tables are provided. This material is available free of charge via the Internet at http://pubs.acs.org.

References

(1) Dirac, P. A. M. *Proc. Cambridge Phil. Soc.* **1930**, *26*, 376–385.

(2) Slater, J. C. *Phys. Rev.* **1951**, *81*, 385–390.

(3) Kohn, W.; Sham, L. J. *Phys. Rev.* **1965**, *140*, A1133–1138.

(4) Hohenberg, P.; Kohn, W. *Phys. Rev.* **1964**, *136*, B864–871.

(5) Parr, R. G.; Yang, W. *Density-Functional Theory of Atoms and Molecules*; Oxford University Press: New York, 1989.

(6) Koch, W. Holthausen, M. *A Chemist's Guide to Density Functional Theory*; Wiley-VCH: Weinheim, Germany, 2001.

(7) Herman, F.; Van Dyke, J. P.; Ortenburger, I. B. *Phys. Rev. Lett.* **1969**, *22*, 807–811.

(8) Becke, A. D. *Phys. Rev. A* **1988**, *38*, 3098–3100.

(9) Perdew, J. P.; Burke, K.; Ernzerhof, M. *Phys. Rev. Lett.* **1996**, *77*, 3865–3868.

(10) Becke, A. D. *J. Chem. Phys.* **1993**, *98*, 5648–5652.

(11) Tao, J.; Perdew, J. P.; Staroverov, V. N.; Scuseria, G. E. *Phys. Rev. Lett.* **2003**, *91*, 146401–146405.

(12) Perdew, J. P.; Zunger, A. *Phys. Rev. B* **1981**, *23*, 5048–5079.

(13) Mori-Sanchez, P.; Cohen, A. J.; Yang, W. *J. Chem. Phys.* **2006**, *124*, 091102.

(14) Iikura, H.; Tsuneda, T.; Yanai, T.; Hirao, K. *J. Chem. Phys.* **2001**, *115*, 3540–3544.

(15) Yanai, T.; Tew, D. P.; Handy, N. C. *Chem. Phys. Lett.* **2004**, *393*, 51–57.

(16) Perdew, J. P.; Ruzsinszky, A.; Tao, J.; Staroverov, V. N.; Scuseria, G. E.; Csonka, G. I. *J. Chem. Phys.* **2006**, *123*, 062201.

(17) Becke, A. D. *Int. J. Quantum Chem.* **1983**>, *23*, 1915–1922.

(18) Becke, A. D.; Roussel, M. R. *Phys. Rev. A* **1989**, *39*, 3761–3767.

(19) Becke, A. D. *J. Chem. Phys.* **2003**, *119*, 2972–2977.

(20) Johnson, E. R.; Becke, A. D. *J. Chem. Phys.* **2005**, *123*, 024101.

(21) Neumann, R.; Nobes, R. H.; Handy, N. C. *Mol. Phys.* **1996**, *87*, 1–36.

(22) Neumann, R.; Handy, N. C. *Chem. Phys. Lett.* **1995**, *246*, 381–386.

(23) Beck, T. L. *Rev. Mod. Phys.* **2000**, *72*, 1041–1080.

(24) Becke, A. D. *Int. J. Quantum Chem. Quantum Chem. Symp.* **1994**, *28*, 625–632.

(25) Bahmann, H.; Ernzerhof, M. *J. Chem. Phys.* **2008**, *128*, 234104.

(26) Katriel, J.; Davidson, E. R. *Proc. Natl. Acad. Sci.* **1980**, *77*, 4403–4406.

(27) Almbladh, C.-O.; von Barth, U. *Phys. Rev. B* **1985**, *31*, 3231–3244.

(28) Tozer, D. J.; Handy, N. C. *J. Chem. Phys.* **1998**, *109*, 10180–10189.

(29) Szabo A. Ostlund, N. S. *Modern Quantum Chemistry, Introduction to Advanced Electronic Structure Theory*; Macmillan: New York, 1982.

(30) Takahashi, H.; Hori, T.; Wakabayashi, T.; Nitta, T. *Chem. Lett.* **2000**, *3*, 222–223.

(31) Takahashi, H.; Hori, T.; Wakabayashi, T.; Nitta, T. *J. Phys. Chem A* **2001**, *105*, 4351–4358.

(32) Hori, T.; Takahashi, H.; Nitta, T. *J. Theoret. Comput. Chem.* **2005**, *4*, 867–882.

(33) Chelikowsky, J. R.; Troullier, N.; Saad, Y. *Phys. Rev. Lett.* **1994**, *72*, 1240–1243.

(34) Chelikowsky, J. R.; Troullier, N.; Wu, K.; Saad, Y. *Phys. Rev. B* **1994**, *50*, 11355–11364.

(35) Barnett, R. N.; Landman, U. *Phys. Rev. B* **1993**, *48*, 2081–2097.

(36) Kleinman, L.; Bylander, D. M. *Phys. Rev. Lett.* **1982**, *48*, 1425–1428.

(37) Ono, T.; Hirose, K. *Phys. Rev. Lett.* **1999**, *82*, 5016–5019.

(38) Frisch, M. J.; Trucks, G. W.; Schlegel, H. B.; Scuseria, G. E.; Robb, M. A.; Cheeseman, J. R.; Montgomery, J. A., Jr.; Vreven, T.; Kudin, K. N.; Burant, J. C.; Millam, J. M.; Iyengar, S. S.; Tomasi, J.; Barone, V.; Mennucci, B.; Cossi, M.; Scalmani, G.; Rega, N.; Petersson, G. A.; Nakatsuji, H.; Hada, M.; Ehara, M.; Toyota, K.; Fukuda, R.; Hasegawa, J.; Ishida, M.; Nakajima, T.; Honda, Y.; Kitao, O.; Nakai, H.; Klene, M.; Li, X.; Knox, J. E.; Hratchian, H. P.; Cross, J. B.; Bakken, V.; Adamo, C.; Jaramillo, J.; Gomperts, R.; Stratmann, R. E.; Yazyev, O.; Austin, A. J.; Cammi, R.; Pomelli, C.; Ochterski, J. W.; Ayala, P. Y.; Morokuma, K.; Voth, G. A.; Salvador, P.; Dannenberg, J. J.; Zakrzewski, V. G.; Dapprich, S.; Daniels, A. D.; Strain, M. C.; Farkas, O.; Malick, D. K.; Rabuck, A. D.; Raghavachari, K.; Foresman, J. B.; Ortiz, J. V.; Cui, Q.; Baboul, A. G.; Clifford, S.; Cioslowski, J.; Stefanov, B. B.; Liu, G.; Liashenko, A.; Piskorz, P.; Komaromi, I.; Martin, R. L.; Fox, D. J.; Keith, T.; Al-Laham, M. A.; Peng, C. Y.; Nanayakkara, A.; Challacombe, M.; Gill, P. M. W.; Johnson, B.; Chen, W.; Wong, M. W.; Gonzalez, C.; Pople, J. A. *Gaussian 03*, revision B.05; Gaussian, Inc.: Pittsburgh, PA, 2003.

(39) Lee, C.; Yang, W.; Parr, R. G. *Phys. Rev. B* **1988**, *37*, 785–789.

(40) DeFrees, D. J.; Levi, B. A.; Pollack, S. K.; Hehre, W. J.; Binkley, J. S.; Pople, J. A. *J. Am. Chem. Soc.* **1979**, *101*, 4085–4089.

(41) Becke, A. D. *J. Chem. Phys.* **1986**, *84*, 4524–4529.

(42) Lieb, E. H.; Oxford, S. *Int. J. Quantum Chem.* **1981**, *19*, 427–439.

(43) Zhang, Y.; Yang, W. *Phys. Rev. Lett.* **1998**, *80*, 890–890.

(44) van Leeuwen, R.; Baerends, E. J. *Phys. Rev. A* **1994**, *49*, 2421–2431.

(45) Pople, J. A.; Head-Gordon, M.; Fox, D. J.; Raghavachari, K.; Curtiss, L. A. *J. Chem. Phys.* **1989**, *90*, 5622–5629.

(46) Curtiss, L. A.; Raghavachari, K.; Redfern, P. C.; Pople, J. A. *J. Chem. Phys.* **1997**, *106*, 1063–1079.

(47) Curtiss, L. A.; Raghavachari, K.; Redfern, P. C.; Pople, J. A. *J. Chem. Phys.* **2000**, *112*, 7374–7383.

(48) Becke, A. D. *J. Chem. Phys.* **1988**, *88*, 1053–1061.

(49) Chase, M. W., Jr.; Davies, C. A.; Downey, J. R.; Frurip, D. J.; McDonald, R. A.; Syverud, A. N. *J. Phys. Chem. Ref. Data* **1985**, *14*, Suppl. No. 1.

(50) Curtiss, L. A.; Raghavachari, K.; Redfern, P. C.; Rassolov, V.; Pople, J. A. *J. Chem. Phys.* **1998**, *109*, 7764–7776.

(51) Jorgensen, W. L.; Chandrasekhar, J.; Madura, J. D.; Impey, R. W.; Klein, M. L. *J. Chem. Phys.* **1983**, *79*, 926–935.

(52) Purvis, G. D., III; Bartlett, R. J. *J. Chem. Phys.* **1982**, *76*, 1910–1918.

(53) Laasonen, K.; Csajka, F.; Parrinello, M. *Chem. Phys. Lett.* **1992**, *194*, 172–174.

CT900416X